ELSEVIER

Soil Dynamics and Earthquake Engineering 20 (2000) 1–15

SOIL DYNAMICS AND EARTHQUAKE ENGINEERING

www.elsevier.com/locate/soildyn

State-of-the-art of geotechnical earthquake engineering practice

W.D.L. Finn[a,b,*]

[a]*Anabuki Chair of Foundation Geodynamics, Kagawa University, 2217-20 Hayashi-cho, Takamatsu City, Kagawa, Japan*
[b]*Civil Engineering Department, University of British Columbia, 2324 Main Mall, Vancouver, BC, Canada V6T 1Z4*

Abstract

Major developments in geotechnical earthquake engineering practice over the last 15 years are reviewed. The objectives of the review are to present a coherent view of the current state of practice at the highest level and to examine trends, which may shape practice in the future. Developments are described in the following areas: specification of design ground motions, dynamic response analysis, evaluation of liquefaction potential, evaluation of residual strength of liquefied soil, post-liquefaction displacement analysis, and seismic risk analysis.

Keywords: Design ground motions; Dynamic response analysis; Liquefaction potential; Residual strength; Post-liquefaction displacement; Seismic risk analysis

1. Introduction

Major developments have occurred in many areas of geotechnical earthquake engineering over the last 15 years. Some of the more important of these developments will be reviewed critically here to provide an understanding of the current state-of-the-art at the highest level of engineering practice. The major areas of practice that are examined are the specification of design ground motions, dynamic response analysis, evaluation of liquefaction potential, evaluation of residual strength of liquefied soil, post-liquefaction displacement analysis, and seismic risk analysis.

The broad coverage of the review precludes a detailed presentation of each development. The reader is presumed to be familiar enough with the area of specialization in which a particular development occurred to appreciate its significance.

2. Specification of design ground motions

2.1. Review of strong motion data

The study and interpretation of the huge volume of strong motion data accumulated in the last decade has greatly clarified our understanding of the seismological and geological parameters that control the recorded response and the variability of ground motions.

There are two important publications, which provide an up-to-date critical evaluation of theoretical and empirical methods for estimating ground motions and the important parameters that control seismic response, which are particularly helpful to geotechnical earthquake engineers. These are a state-of-the-art paper by Somerville [1] on ground motions and the January/February 1997 special issue of Seismological Research Letters published by the Seismological Society by America [2] dealing with attenuation relations for ground motions. These reports form the basis for the general review of ground motions given below.

The seismic motions for design are usually specified by a response spectrum. The spectrum is based on a probabilistic seismic hazard analysis and represents ground motion having a specified annual probability of exceedence. The modern trend is to base design on an equal hazard spectrum, that is, a spectrum that has an equal probability of exceedence at all periods. In Eurocode 8 [3] the design spectrum has a probability of exceedence of 10% in 50 years corresponding to a probability of 1/475. There are plans in the USA for implementing an annual probability of exceedence of 2% in 50 years in the Uniform Building Code [4].

A major problem in determining equal hazard spectra by probabilistic analysis is characterizing the variability in ground motions. Two types of uncertainty in ground motion estimates have been identified; aleatory uncertainty due to the random nature of response to earthquakes and epistemic

* Anabuki Chair of Foundation Geodynamics, Kagawa University, 2217-20 Hayashi-cho, Takamatsu City, Kagawa, Japan. Tel.: +81-87-864-2170; fax: +81-87-864-2003.

E-mail address: finn@civil.ubc.ca (W.D.L. Finn).

0267-7261/00/$ - see front matter
PII: S0267-7261(00)00033-6

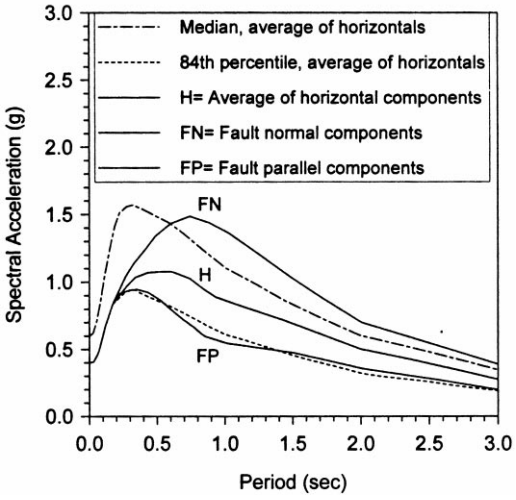

Fig. 1. Response spectra for forward directivity conditions for a $M = 7$ earthquake at a distance of 5 km on soil. Response spectra are shown for strike-normal, strike-parallel and average horizontal components (after Somerville and Graves [8]).

uncertainty, which is due to our lack of knowledge of the processes linking a seismic event to a resulting ground motion at a site. More research and more data can reduce epistemic uncertainty, but the aleatory uncertainty remains. At the practical level, two important sources of variability have been identified by Abrahamson and Youngs [5]. One is the variability of average ground motions from one event to the next, and the other is the variability in ground motions between sites equidistant from the earthquake in a given event. Youngs et al. [6] found that for crustal earthquakes larger than $M = 6$, the event to event variability was insignificant compared to the intra-event variability.

A key element in seismic hazard analysis is the ground motion model or attenuation relation. Variation of ground motion parameters about the mean attenuated motions are usually assumed to be log-normally distributed. In the past, these attenuation relationships were based on magnitude, distance and site category. However, in the last decade attenuation laws have been developed that include other parameters, which are now known to be significant. These include the tectonic environment, style of faulting and the effects of topography, deep basin edges and rupture directivity.

Three main tectonic environments give significantly different ground motion characteristics: shallow crustal earthquakes in tectonically active regions, shallow crustal earthquakes in tectonically stable regions, and subduction zone earthquakes. These distinctions are recognized and applied in practice in North America and New Zealand, but ignored in most other regions of the world [1].

Ground motion data suggest that ground motions depend, in a significant way, on the style of faulting. Ground motions from reverse faulting may be up to 20% greater than from strike slip earthquakes, and those from normal faulting may be up to 20% lower than those from strike slip earthquakes. Somerville and Sato [7] suggest that these differences may be related to the rise time of slip on the fault.

Near fault ground motions are strongly affected by directivity. Ground motions in Kobe, within 5 km of the fault, showed a ratio of more than 2 to 1 between strike normal and strike parallel ground motion components. The motions propagated along the fault towards Kobe and there were strong directivity effects. Forward directivity occurs when both the rupture and the direction of slip on the fault are towards the site. These conditions are usually met in strike slip faulting. Forward directivity increases the level of spectral response of the strike normal component for periods longer than 0.5 s. Backward directivity effects occur when the rupture propagates away from the site and has the opposite effect. In this case, the longer period motions have lower amplitudes. The conditions for forward directivity are also met in both reverse and normal faulting. The rupture directivity effects from these deep slip faults are produced at sites located around the surface exposure of the fault. Somerville and Graves [8] developed modifications to empirical ground motion attenuation relations to account for the effects of directivity. They show empirical response spectra for forward directivity for a $M = 7$ earthquake at 5 km distance on soil (Fig. 1). These spectra are generated by modifying the empirical median and 84th percentile response spectra predicted by Abrahamson and Silva [9].

Directivity effects are taken into account in the design of retrofits for the California Transportation Authority (CALTRANS) toll bridges by using separate response spectra with a strike normal and strike parallel components to represent near-fault effects.

Evidence from recorded strong motion data indicates that ground motions may be large at the edges of fault controlled basins. For example, strong motion recordings in the Santa Monica area from the 1994 Northridge earthquake are characterized by large amplitudes and durations of shaking. In this region, the basin edge geology is controlled by the active strand of the westward striking Santa Monica fault. Despite having similar surface geology, sites to the north of the fault show relatively modest amplitudes, whereas sites to the south of the fault exhibit significantly larger amplitudes, with a clear and immediate increase in amplification occurring at the fault scarp. Graves et al. [10] used 2D and 3D finite difference ground motion simulations to investigate the significance of the basin-edge structure.

2.2. Selection of design ground motions

It is currently fashionable to develop design spectrum compatible time histories. This development entails the modification of a time history so that its response spectrum matches within a prescribed tolerance level, the target design spectrum. In such matching it is important to retain the phase characteristics of the selected ground motion time history. Many of the techniques used to develop compatible motions do not retain the phase. Abrahamson [11] has

developed an approach that does preserve the phasing of the original record.

The response spectrum alone does not adequately characterize near-fault ground motion. This motion is usually characterized by a long period pulse of strong motion of a fairly brief duration rather than the stochastic process of long duration that characterizes more distant ground motions. Spectrum compatible motions will not have this characteristic unless the basic motion being modified to ensure compatibility has forward directivity effects included.

Spectral compatible motions match the entire spectrum within a prescribed tolerance. No real earthquake ground motions will do this. It has been common in the seismic design of critical structures to select representative earthquakes in the near-field, intermediate-field and far-field with a view to exploring the full range of spectral response in the structure. However, when spectral compatible motions are used, all periods are subjected to the full design seismic action. Naeim and Lew [12] on the basis of nonlinear analysis of structures have expressed the view that these spectrum compatible motions should not be used for damage assessment because they give exaggerated estimates of displacement demand and energy input. For this reason, designers should be cautious about using spectrum compatible motions when estimating the displacements of embankment dams and earth structures under strong shaking, if the acceptable performance of these structures is specified by criteria based on tolerable displacements. Representative recorded earthquake motions that match different parts of the spectrum are preferable.

2.3. Special cases

In most existing attenuation relationships, there is no explicit recognition of directivity effects. These effects tend to contribute to some of the substantial deviations from the median ground motions. If the probabilistic response spectrum is based on median ground motions, then it likely represents average directivity conditions. If the response is based on the mean plus one standard deviation, then it approximates forward directivity conditions and many of the time histories used should have forward directivity characteristics [1].

One of the difficulties with designs based on spectra is determining what are the appropriate scenario earthquakes for selecting appropriate recorded ground motions for nonlinear analyses or for conducting liquefaction analyses. The probabilistic response spectrum represents the aggregated contribution of a range of earthquake magnitudes on different faults and seismic zones at various distances from the site, and also includes the effect of random variability for a given magnitude and distance. Appropriate earthquakes can be determined using a procedure proposed by McGuire [13], which deaggregates the contributions to the spectrum by magnitude, distance and the parameter ϵ that, for the deaggregated magnitude and distance, defines the number of standard deviations above or below the median ground motion level that is required to match the probabilistic spectrum.

In the near-fault region, the horizontal ground motion in the direction perpendicular to the fault strike is significantly larger than the horizontal component parallel to the fault strike at periods longer than about 0.5 s. Since fault strike is usually well known close to major faults, it is straightforward to take the difference between the strike normal and strike parallel components of motion into account in the evaluation of near-fault ground motions, especially for base isolated buildings, bridges, dams, and other structures that are particularly sensitive to long-period ground motions. Consideration of these differences may be especially important for the retrofit of existing structures near active faults.

Foundations of long structures such as the multiple supports of a bridge undergo different ground motions at each support. To properly evaluate the response of such structures, it is necessary to vary the ground motions across the foundation. There are two effects that need to be considered; the wave passage effect and the lack of coherence between the motions at the different locations. The incoherence increases with increasing distance between the supports and increases in the wave frequencies.

Abrahamson et al. [14] developed models of spatial variation of ground motion from strong motion data recorded in dense arrays. Abrahamson has also developed methods for generating suites of time histories for different foundation locations with spatial incoherence that matches the prescribed coherency model.

3. Dynamic response analysis

The dynamic response analysis of earth structures and soil sites is still largely based on technology developed in the 1970s and which represents the very first attempts to carry out nonlinear analysis by equivalent linear (EQL) procedures.

The EQL analyses are conducted in terms of total stresses and so the effects of seismically induced porewater pressures are not reflected in the computed stresses and accelerations. Also since the analyses are elastic, they cannot predict the permanent deformations directly. Therefore equivalent linear methods are used only to get the distribution of accelerations and shear stresses in the dam. Semi-empirical methods are used to estimate the permanent deformations and porewater pressures using the acceleration and stress data from the equivalent linear analyses [15]. Finn [16] has presented a detailed review of these methods.

These procedures appear to work quite well provided the behavior of the structure is not strongly nonlinear and significant pore pressures do not develop. Seed et al. [17] note that this method can occasionally predict large

displacements that do not occur, when there is strong nonlinearity or high porewater pressures. The Newmark [18] analysis procedure based on sliding rigid block analysis, which is often used in practice, is particularly inappropriate when a large zone has liquefied in an embankment or foundation.

A major motivation for the development of more general constitutive relations has been the need to model nonlinear behavior in terms of effective stresses and to provide reliable estimates of porewater pressures and permanent deformations under seismic loading.

A hierarchy of constitutive models is available for the dynamic response of embankment dams to earthquake loading. The models range from the relatively simple hysteretic nonlinear models to complex elastic–kinematic hardening plasticity models. Detailed critical assessments of these models may be found in Finn [16,19] and Marcuson et al. [20].

3.1. Direct nonlinear analysis

The direct nonlinear approach is presented as incorporated in the program TARA-3 [21] because there is extensive experience in using this method in practice. In addition, the program has been validated in an extensive series of centrifuge tests conducted on behalf of the US Nuclear Regulatory Commission [19].

In this model, the behavior of soil in shear is assumed to be nonlinear and hysteretic. The response of the soil to uniform all round pressure is assumed to be nonlinearly elastic and dependent on the mean normal effective stress.

The objective during analysis is to follow the stress–strain curve of the soil in shear during both loading and unloading. Checks are built into the program to establish whether or not a calculated stress–strain point is on the stress–strain curve and correction forces are applied to bring the point back on the curve if necessary. To simplify the computations, the stress–strain curve is assumed to be hyperbolic. This curve is defined by two parameters, which are fundamental soil properties, the strength τ_{max} and the in situ small strain shear modulus G_{max}.

The response of the soil to an increment in load, either static or dynamic, is controlled by the tangent shear and tangent bulk moduli appropriate to the current state of the soil. The moduli are functions of the level of effective stress and therefore excess porewater pressures must be continually updated during analysis, and their effects on the moduli taken progressively into account.

During seismic shaking, two kinds of porewater pressures are generated in saturated soils; transient and residual. The residual porewater pressures are due to plastic deformations in the sand skeleton. These persist until dissipated by drainage or diffusion and therefore they exert a major influence on the strength and stiffness of the soil skeleton. These pressures are modeled in TARA-3 using the Martin et al. [22] porewater pressure model.

In the past decade, this type of analysis has been widely used in seismic safety evaluation of embankment dams and in assessing remediation options using displacement criteria.

3.2. Elastic–plastic methods

The more appropriate elastic–plastic models of soil behavior under cyclic loading are based on a kinematic hardening theory of plasticity based on multi-yield surfaces or a boundary surface theory with a hardening law giving the evolution of the plastic modulus. These constitutive models are complex and incorporate some parameters not usually measured in field or laboratory testing. Soil is treated as a two-phase material using coupled equations for the soil and water phases. The coupled equations and the more complex constitutive models make heavy demands on computing time [16].

Validation studies of the elastic–plastic models suggest that, despite their theoretical generality, the quality of response predictions is strongly path dependent [16,23]. When loading paths are similar to the stress paths used in calibrating the models, the predictions are good. As the loading path deviates from the calibration path, the prediction becomes less reliable.

Typical elastic–plastic methods used in practice to evaluate the seismic response of embankment dams are DYNAFLOW [24], DIANA [25], DSAGE [26], DYNARD [27], and FLAC [28].

3.3. Recommendations for analysis

Analysis should be conducted in the appropriate stress mode, either total stress or effective stress. Reliable programs, which are adequately validated, are available to conduct such analyses. However, no matter which program is used, it is vitally important to calibrate the constitutive model for the job at hand. The stress–strain features of the model should be calibrated for the dominant loading path expected. If this is primarily shear on horizontal planes, then calibration is best done in terms of simple shear data. If rocking is of prime concern, then triaxial test data would be preferable. Different calibrations may be necessary for different parts of the region being analyzed. Calibration for seismic loading should include the use of cyclic loading data either from simple shear or triaxial tests. It has been well documented in the past [23] that calibration using static test data does not lead to good predictions of response to cyclic loading.

It is especially important to calibrate the porewater pressure prediction process. If in-situ penetration test data, such as SPT or CPT data is used to establish the liquefaction resistance curve for design, then the constitutive model should be able to predict the curve. If laboratory data from high quality samples are available, then the rate of development of porewater pressure during cyclic loading should be adequately predicted by the calibrated model.

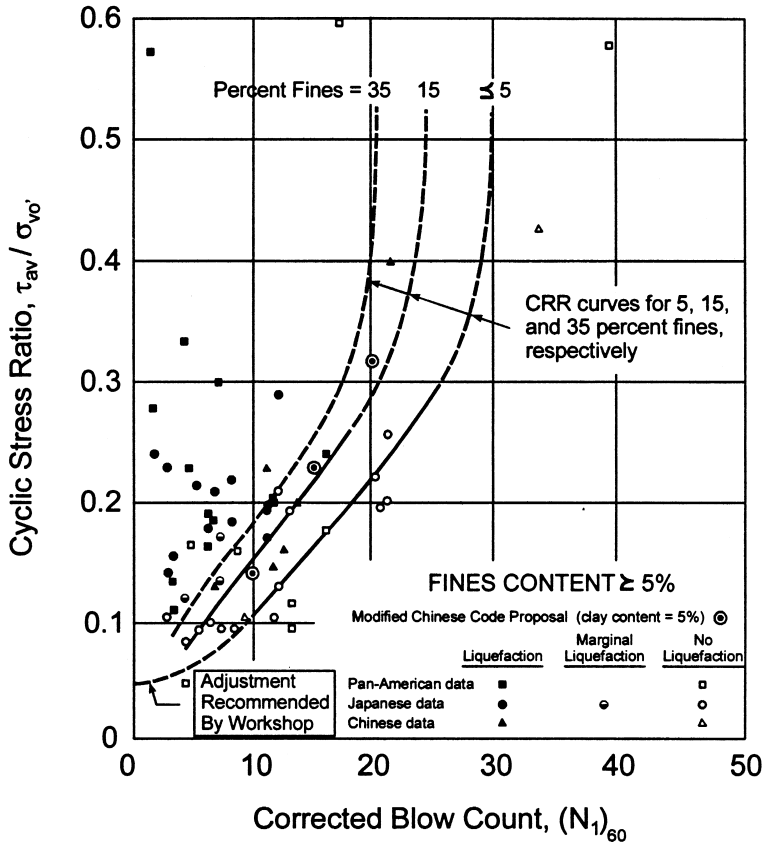

Fig. 2. Simplified base curve recommended for calculation of CRR from SPT data along with empirical liquefaction data (modified from Seed et al. [31]).

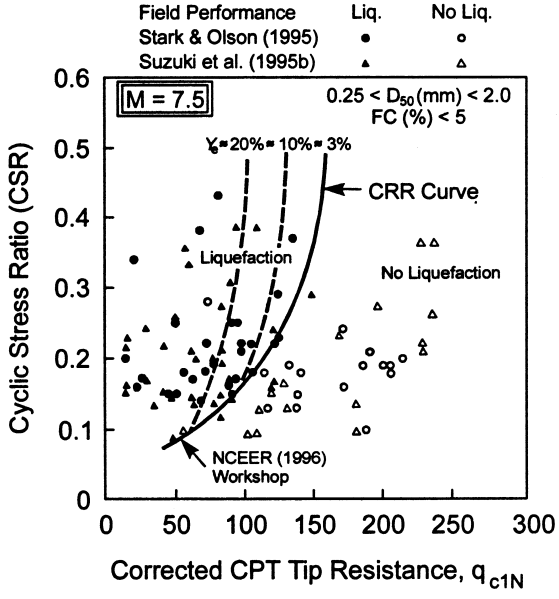

Fig. 3. Curve recommended for calculation of CRR for earthquake magnitude $M = 7.5$ from CPT data along with empirical liquefaction data (modified from NCEER [30]).

This type of performance calibration puts useful restraints on the operation of the constitutive model and gives rise to more confidence in the computed response of the structures. Such calibration should be conducted in cooperation with an engineer with extensive experience in determining soil properties and in interpreting in-situ field data.

4. Liquefaction

Procedures for evaluating liquefaction were studied by a committee appointed by the National Centre for Earthquake Engineering Research at the University of Buffalo in 1996. The objective was to review research and field experience on liquefaction since 1985 when a similar committee reported on the state-of-the-art [29] and recommended standards for practice. The findings of the NCEER committee may be found in a report edited by Youd and Idriss [30].

The liquefaction-resistance chart proposed by Seed et al. [31] in 1985, as a standard for practice, was modified slightly by the NCEER committee. In the original chart, the line of critical stress ratios for a $M = 7.5$ earthquake passed through the origin. In the revised chart, the lower part of this curve cuts the stress ratio axis at 0.05 as shown in Fig. 2.

The NCEER committee also recommended a liquefaction

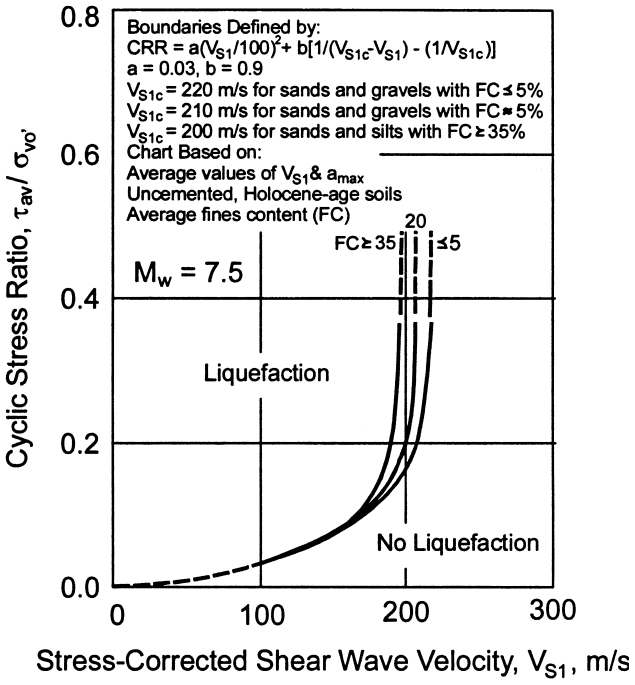

Fig. 4. Curves recommended by workshop for calculation of CRR from corrected shear wave velocity (modified from NCEER [30]).

assessment chart based on cone penetration test data shown in Fig. 3. Since 1985, the volume of cone penetration data available for analysis increased greatly and there is now sufficient CPT data to define the critical stress ratio curve separating liquefaction conditions from non-liquefaction conditions. Earlier, liquefaction resistance charts using CPT data were based heavily on SPT data converted to equivalent CPT data.

Another significant change recommended by the NCEER committee is the adoption of the Robertson and Fear [32] procedure for evaluating liquefaction potential using the cone penetration test. They developed a unified approach for interpreting cone data for liquefaction assessment without direct determination of the fines content. The procedure is based on a soil chart, which identifies the soil type on the basis of normalized cone bearing resistance and normalised side friction.

The NCEER committee recommended a liquefaction assessment chart based on shear wave velocity (Fig. 4). As shown in Fig. 5, this chart is radically different from the chart advocated by Eurocode 8.

The chart proposed by Eurocode 8 is one that was developed by Robertson et al. [33]. This chart was based on limited data. A great deal of data has become available since that time and this has led to the very different recommendation by NCEER [30].

The NCEER committee reviewed the magnitude correction factors used to convert the critical stress ratios from the liquefaction assessment chart for $M = 7.5$ to those appropriate for earthquakes of other magnitudes. They adopted new factors proposed by Idriss [34], which are given in the NCEER [30] report. These factors are shown in Table 1 where they are compared with factors developed by Ambraseys [35] on the basis of field data available up to about 1986, and the factors recommended by Seed and Idriss, which are based substantially on laboratory data. The new factors are significantly higher than the factors recommended by Seed and Idriss [36].

The factor K_σ which corrects the stress ratio corresponding to $(N_1)_{60}$ for the effects of effective overburden pressure has been revised substantially (Fig. 6). The greatest

Table 1
Magnitude scaling factor values defined by various investigators (after NCEER [30])

Magnitude (M)	Seed and Idriss [30]	Idriss [34]	Ambraseys [35]
5.5	1.43	2.20	2.86
6.0	1.32	1.76	2.20
6.5	1.19	1.44	1.69
7.0	1.08	1.19	1.30
7.5	1.00	1.00	1.00
8.0	0.94	0.84	0.67
8.5	0.89	0.72	0.44

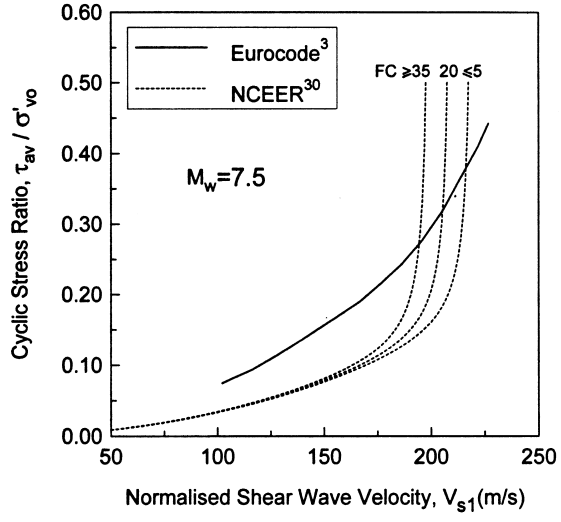

Fig. 5. Comparison of NCEER [30] and Eurocode 8 [3] recommendations for evaluation of liquefaction potential on the basis of wave velocity.

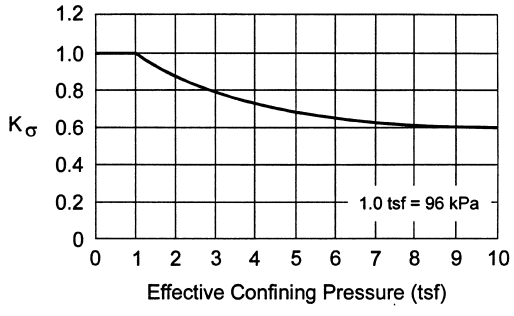

Fig. 6. Minimum values for K_σ recommended for clean and silty sands and gravels (modified from NCEER [30]).

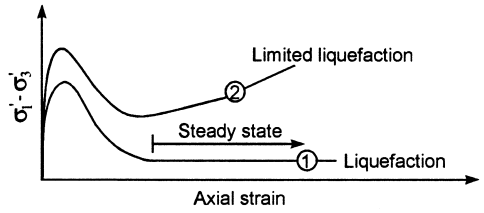

Fig. 7. Types of contractive deformation.

reduction factor due to overburden pressure is now 0.6; previously it went as low as 0.4.

Since the NCEER report was published, the committee has continued to meet to consider the impact of more recent research on the recommendations of the report. If further modifications are made, they will be reported in a summary paper on the NCEER report being prepared for publication in the Geotechnical Journal of the American Society of Civil Engineers.

5. Residual strength

In the context of this review, liquefaction is synonymous with strain softening of relatively loose sands in undrained shear as illustrated by curve 1 in Fig. 7. When the sand is strained beyond the point of peak strength, the undrained strength drops to a value that is maintained constant over a large range in strain. This is conventionally called the undrained steady state or residual strength. If the strength increases after passing through a minimum value, the phenomenon is called limited or quasi-liquefaction and is illustrated by curve 2 in Fig. 7. Even limited liquefaction may result in significant deformations because of the strains necessary to develop the strength to restore stability.

A major challenge facing engineers is the selection of the appropriate residual strength of liquefied materials for use in analyses to assess the post-liquefaction stability of embankments and other soil structures. The residual strength has a major impact on the cost of remediation. Laboratory research, especially in the last 5 years, has done much to clarify the factors that control residual strength and provides some basis for selecting residual strength for design. However, the appropriate residual strength for design and analysis is still controversial.

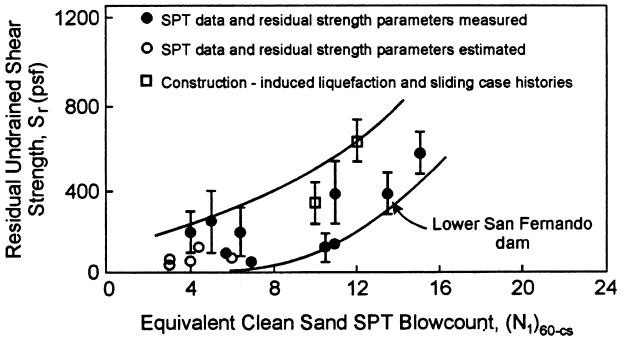

Fig. 8. Relationship between corrected "clean sand" blowcount $(N_1)_{60\text{-cs}}$ and undrained residual strength, s_r, from case studies (after Seed and Harder [38]).

5.1. Residual strength based on case histories

Seed [37] back-analyzed a number of embankments in which significant displacements had occurred during earthquakes as a result of liquefaction. He published a chart linking the residual strength to the $(N_1)_{60\text{-cs}}$, the normalized penetration resistance for clean sands. A revised version of this chart by Seed and Harder [38] is shown in Fig. 8. Use of this chart for estimating residual strength is widespread in engineering practice.

Concerns have been expressed that in some case histories in Fig. 8, displacements may not have been sufficient to have mobilized residual strength. In others, because of lack of direct data, either assumptions or data from adjacent locations had to be used to generate the appropriate $(N_1)_{60\text{-cs}}$. There seem to be very few case histories for clean sand in the correlation. The correction for fines content has also been queried. Recently, the National Science Foundation held a workshop on residual strength at which these questions were discussed [39]. A committee has been appointed to re-examine these case histories and to report in due course. This report should be of great interest and may result in proposed changes to the correlation. It is hoped that the review will also provide the data to facilitate independent interpretation of the case histories.

Another limitation of the analysis of field data is the assumption that sliding takes place on a single slip surface as in conventional slope stability analysis. This assumption is not valid when a significant liquefied zone is deforming. Energy is dissipated throughout the deforming liquefied zone. The only way to capture this energy dissipation is by a finite element analysis that incorporates the proper distribution of residual strength. Neglecting the volumetric dissipation of energy is analogous to ignoring the zones of radial shear AGC and BCD in the classical Prandtl solution for undrained bearing capacity of a clay (Fig. 9) and assuming shear is mobilized only on the bounding sliding surfaces such as ACDE and FGCB. If the zones of radial shear are neglected, the estimated bearing capacity is $4.36c_u$ which is 85% of the Prandtl value of $5.14c_u$, where c_u is the undrained shear strength.

6. Residual strength from laboratory tests

Extensive research has been conducted in the laboratory on the factors controlling the residual strength. Originally, it was thought to be a function only of the void ratio for a given sand [40,41]. Research studies, since 1988, some of which will be described below, suggest that the undrained

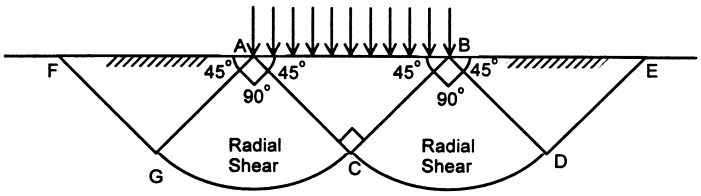

Fig. 9. Failure mechanism under a long footing in clay.

residual strength measured within the strain capacity of laboratory equipment is a function of:

- sample preparation technique;
- stress path followed during loading;
- effective confining pressure.

6.1. Effect of sample preparation

Many laboratory studies of liquefaction use samples prepared by moist tamping because it is the easiest way to form relatively loose samples. However, it frequently results in void ratios, which are not accessible to the same sand under deposition conditions in the field. Other methods in use are air pluviation and pluviation under water. Vaid et al. [42] has demonstrated that the residual strength measured on samples prepared in different ways are quite different (Fig. 10). Vaid et al. [43] tested frozen field samples of two different Recent sands to determine the residual strength. He then reconstituted the same samples to the same void ratio using pluviation in water. The reconstituted samples gave residual strengths very similar to the frozen field samples. These results are a strong argument for using pluviation under water to form representative samples of soils, which were originally deposited under water or were placed by hydraulic fill construction. The moist tamping method would seem to be more appropriate for forming representative samples of unsaturated compacted soils.

6.2. Stress path

Uthayakumar and Vaid [44] and Yoshimine et al. [45] have explored the effects of stress path on residual strength over a wide range of stress paths defined by α, the inclination of the principle stress to the vertical axis of the sample, and the parameter $b = (\sigma_2 - \sigma_3)/(\sigma_1 - \sigma_3)$, which is a measure of the intermediate principle stress. The samples were tested using the hollow cylinder torsional shear device. Typical examples of this kind of data [45] are shown in Fig. 11, which suggest that different residual strengths should be assigned to different parts of a liquefied zone in an embankment depending on the predominant stress conditions. This selective use of shear strength for design is not new. Bearing capacity under offshore structures in the North Sea is evaluated using compression, simple shear and extension strength data to suit stress conditions at different locations along potential sliding surfaces.

6.3. Residual strength as a function of effective confining pressure

The practice of expressing the residual strength as a fraction of the effective confining pressure has been used in practice on several water-retaining and tailings dams since it was used on Sardis Dam in 1989 [46,47]. For the most part, the ratio selected has been between 0.06 and 0.1. A value of $S_r/p' = 0.23$ was used for Duncan Dam, based on extensive testing of frozen samples [48].

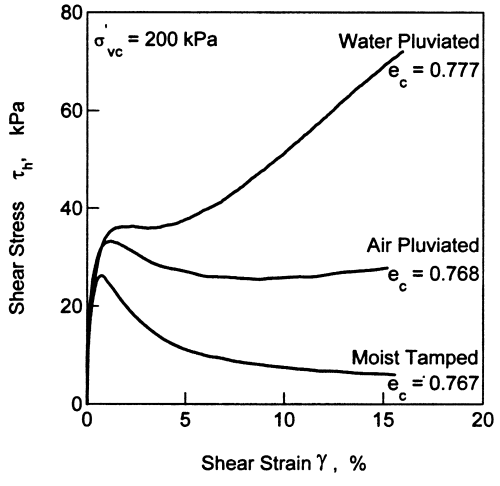

Fig. 10. The effect of sample preparation on undrained simple shear response of Syncrude sand (Vaid et al. [42]).

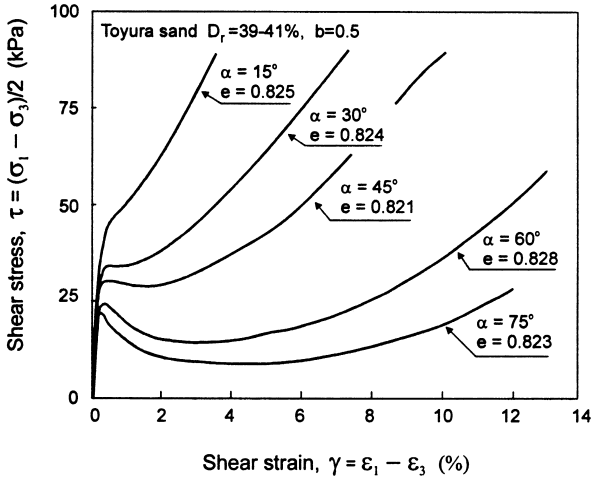

Fig. 11. Effect of stress path on undrained behavior of Toyoura sand (Yoshimine et al. [45]).

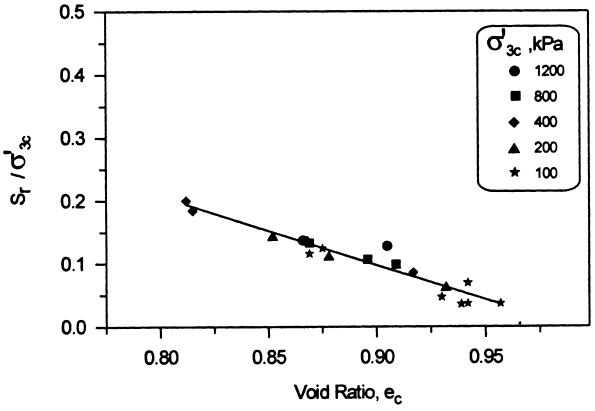

Fig. 12. Relationship between the residual strength normalized by the effective confining stress and void ratio in extension tests on Fraser River (after Vaid and Thomas [49]).

Vaid and Thomas [49], using extension tests with frictionless end platens, determined the residual strength of Fraser River sand over a range of void ratios and confining pressures. The results clearly demonstrated the dependence of residual strength of overburden pressure. Their results are replotted in Fig. 12; normalized with respect to the effective confining stress. Despite some scatter, the variation of S_r/p' is well represented by the curve shown (Fig. 12). Similar results (Fig. 13) were obtained for simple shear tests by Vaid and Sivathayalan [50].

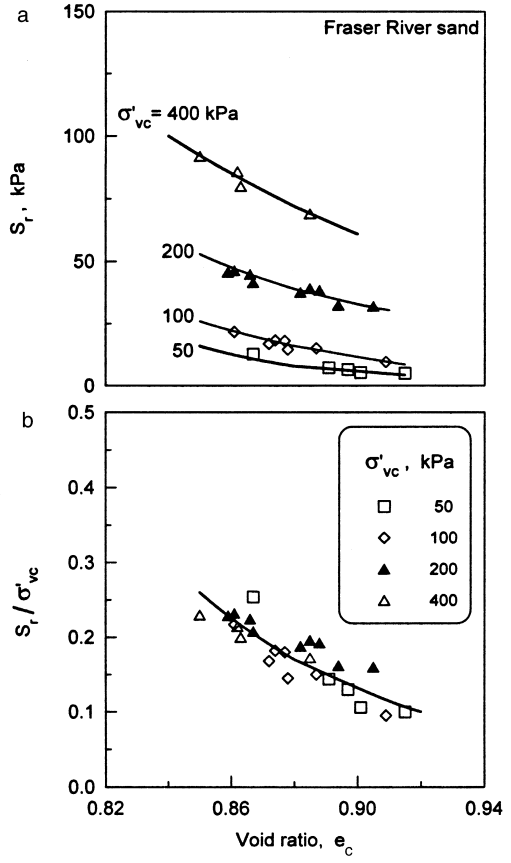

Fig. 13. (a) Variation of steady-state strength in simple shear with void ratio and confining stress, (b) Variation of normalized residual strength with void ratio (after Vaid and Sivayathalan [50]).

7. Post-liquefaction displacement analyses

The use of large displacement analysis in evaluating post-liquefaction response and assessing the adequacy of proposed remediation measures has now become part of engineering practice. It was first applied to Sardis Dam in 1989 by Finn et al. [47]. Post-liquefaction analysis and its application in design of remediation measures have been the subject of previous reviews [16,51]. Practice has demonstrated that remediation measures based on displacement criteria are much more cost-effective than those based on the factor of safety approach.

There has been little direct validation of displacement analysis based on field data. The few case histories available are poorly defined, both in terms of input motion and in the definition of the deformed shape of the dam. A large number of embankment failures, which occurred in Hokkaido during the Kushiro-oki earthquake of 1993 and the Nansei-oki earthquake of 1994, provided a good opportunity for validating post-liquefaction deformation analysis by means of a series of blind tests in which predictions were checked against field data by an independent group. These case histories will be described below in some detail because of their importance for the validation of displacement analysis.

Between 1995 and 1998, displacement analyses were conducted on many flood protection dikes in Hokkaido, Japan, which had been damaged during the Kushiro-oki and Nansei-oki earthquakes in 1993 and 1994, respectively. The objective was to develop a criterion based on potential post-liquefaction crest settlement to prioritize the remediation of dikes against future earthquakes. A two-step strategy was adopted for the studies. First, failures of dikes in eastern Hokkaido would be simulated. If these simulations were satisfactory, then the analyses would be used to predict crest settlements in a number of dikes in western Hokkaido, which had significant post-liquefaction displacements. The displacement analyses were conducted in Vancouver, Canada, and the predictions were verified by engineers from the Advanced Construction Technology Center (ACTEC), Tokyo, and the Hokkaido Development Bureau on the basis of field data known only to them.

7.1. Simulation of dike failure at section 9K850 in eastern Hokkaido

The failure mode at a location on the left bank of the Kushiro river is shown in Fig. 14. The height of the dike before the earthquake was about 7 m and the crest width was about 8 m. As a result of earthquake shaking, the crest of the

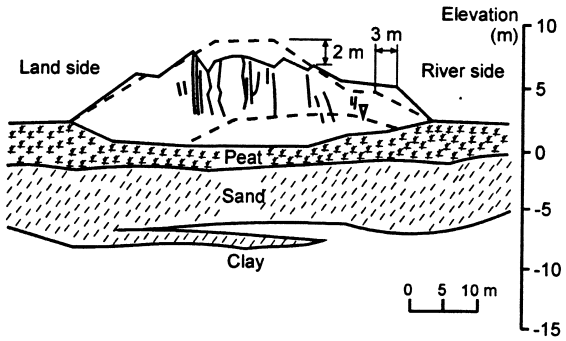

Fig. 14. Mode of failure on left bank of Kushiro River at station 9K850.

dike settled about 2 m and movement of the slope of the order of 3 m took place towards the river. The ground was frozen to a depth of about 0.7 m at the time of the earthquake. The brittle nature of the frozen layer is probably responsible for the sharp step feature in the crest near the upstream slope. This frozen layer was taken into account during the simulation.

Appropriate input motions for seismic analysis were specified by Jishin Kogaku Kenkyusho, Tokyo. Relevant soil properties were provided by ACTEC. Dynamic analysis was conducted in the effective stress nonlinear mode using the program TARA-3 [21]. The large strain post-liquefaction deformations were calculated using the program TARA-3FL [52]. This program allows the liquefied region to deform at constant volume and uses a Lagrangian updating scheme to handle large strains.

The computed deformed shape of the dike is shown in Fig. 15. The sharp break in the surface shows the effect of the frozen ground. The deformed shape and the magnitudes of displacements agree fairly well with the displacements measured after the earthquake. The computed maximum settlement and horizontal displacement are 2.3 and 2.7 m, respectively, compared to measured displacements of 2 and 3 m.

The simulation studies were considered satisfactory and a major parametric study was approved to investigate the effects of some of the important cross-sectional parameters that control the consequences of liquefaction, such as the thickness of a non-liquefiable layer overlying the liquefied layer, the thickness of the liquefied layer itself, and the

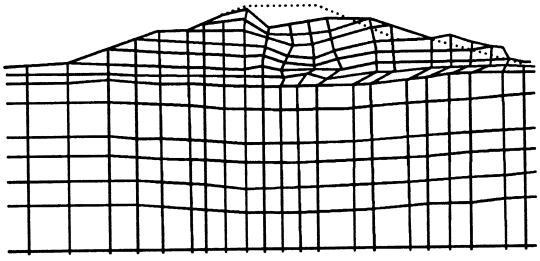

Fig. 15. Computed post-liquefaction shape of the dike.

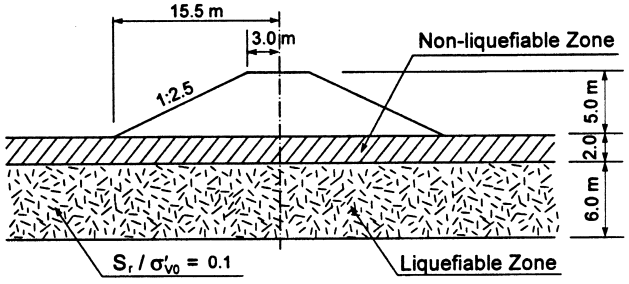

Fig. 16. Typical cross-section of dike for analysis.

height and side slopes of the dikes. The effects of these parameters were characterized by the settlements of the crests of the dikes after liquefaction.

7.2. Estimation of crest settlements

The crest settlements were estimated first for dikes with side slopes 1:2.5 as shown in Fig. 16. The thicknesses of the liquefied and non-liquefied layers were varied and the resulting displacements after liquefaction are plotted in non-dimensional form in Fig. 17.

The non-dimensional computed crest settlements, S/H_D are shown by the curve in Fig. 17. The equation of the curve is given by:

$$\frac{S}{H_D} = 0.01 \exp\left(0.922 \frac{H_D}{H_{NL}} \frac{H_L}{H_{NL}}\right) \quad (1)$$

where S is the crest settlement, H_D the height of the dike; H_L and H_{NL} are the thicknesses of the liquefiable and non-liquefiable layers, respectively. The residual strength ratio was $S_r/\sigma'_{vo} = 0.10$. This curve was adopted for predicting crest settlement.

Engineers from ACTEC and the Hokkaido Development Bureau compared the measured crest settlements from a wide variety of dikes in western Hokkaido, which underwent noticeable displacements during the Nansei-oki

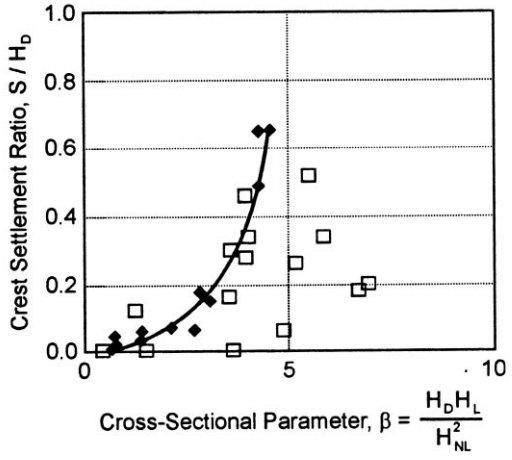

Fig. 17. Comparison of crest settlement prediction curve for dikes with slopes 1:2.5 with actual crest settlements for dikes with various side slopes.

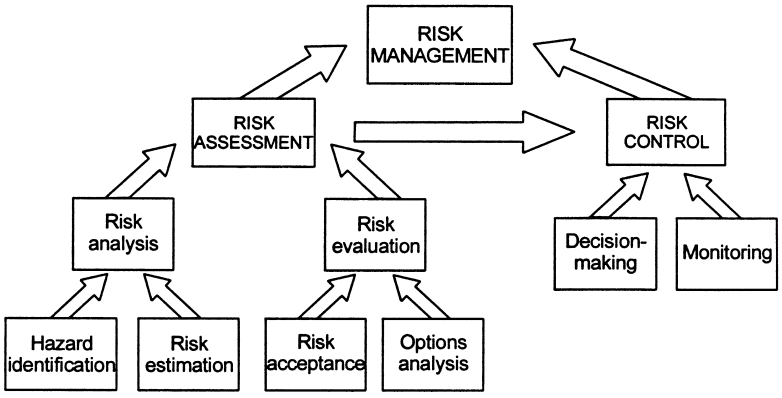

Fig. 18. Risk management framework proposed by Canadian Standards Association (from International Journal on Hydropower and Dams [60] with permission).

earthquake in 1994 with those predicted by Eq. (1). The data points and the prediction curve are plotted in Fig. 17. The black points represent the real cases corresponding to some of the idealized analyses done to develop the curve; the open points represent other dikes. The agreement was very good for dikes with slopes of 1:2.5, but the field data showed that the side slopes had an important effect on the crest settlement and that separate criteria would be necessary for two other predominant slopes; uniform side slopes of 1:5, and unequal slopes, 1:5 and 1:10. Parametric studies were conducted for different values of S_r/σ'_{vo}. Displacements in dikes with $S_r/\sigma'_{vo} \geq 0.15$ were all within the tolerable range. It can be seen that the criterion based on crest settlement can be useful for deciding which dikes should be remediated first. The larger the predicted settlement, the more urgent the need for remediation. The Hokkaido dikes study is an important case history because it is the only instance in which post-liquefaction displacement analysis has been validated independently in blind tests in a large number of earth structures undergoing different levels of post-liquefaction displacements.

8. Seismic risk in geotechnical earthquake engineering

8.1. Seismic risk assessment for dams

Seismic risk analysis provides a rational basis for the evaluation of dam safety during an earthquake. It is a process by which the consequences of exposure to a range of probabilistic seismic hazards are determined. The consequences are most often expressed in terms of both loss of life or economic loss at various probabilities of exceedence.

Risk analysis in the field of embankment dams is relatively new in engineering practice and most engineers do not have the knowledge or experience for making decisions on the basis of risk assessment. Risk assessment was adopted by the US Bureau of Reclamation (USBR) in 1995 and the US Army Corps of Engineers in 1997. The objective of USBR was "to ensure that structures do not create unacceptable risks to public safety and welfare, property, the environment and cultural resources". The Canadian Standards Association has developed the general framework for risk management shown in Fig. 18. There are two main structures in the framework, risk assessment and risk

Table 2
Usual minimum criteria for design earthquakes [53]

	Minimum design earthquake (MDE)[a]	
Consequence category	Deterministically derived	Probabilistically derived (Annual exceedence probability)
Very high	MCE[b]	10^{-4}
High[c]	50% to 100% MCE	10^{-3} to 10^{-4}
Low	–	10^{-2} to 10^{-3}

[a] MDE (maximum design earthquake) firm ground accelerations and velocities can be taken as 50–100% of MCE values. For design purposes the magnitude should remain the same as the MCE.

[b] For a dam site, MCE (maximum credible earthquake) ground motions are the most severe ground motions capable of being produced at the site under the presently known or interpreted tectonic framework.

[c] In the 'High' consequence category, the MDE is based on the consequences of failure. For example, if one incremental fatality would result from failure an AEP (annual exceedence probability) of 10^{-3} could be acceptable, but for consequences approaching those of a 'Very High' consequence dam, design earthquakes approaching the MCE would be required.

Table 3
Consequence classification of dams [53]

Consequence	Potential incremental consequences of failure[a]	
	Loss of life	Economic, social, environmental
Very high	Large increase expected[b]	Excessive increase in social, economic and/or environmental losses.
High	Some increase expected[b] Substantial increase in social, economic and/or environmental losses.	
Low	No increase expected	Low social, economic and/or environmental losses.
Very low	No increase	Small dams with minimal social, economic and/or environmental losses. Losses generally limited to the owner's property; damages to other property are acceptable to society.

[a] Incremental to the impacts, which would occur during an earthquake but without failure of the dam. The type of consequence (e.g. loss of life or economic losses) with the highest rating, determines which category is assigned to the structure.

[b] The loss-of-life criteria which separate the 'High' and 'Very High' categories may be based on risks which are acceptable or tolerable to society, taken to be 0.001 lives per year for each dam. Consistent with this tolerable societal risk, the minimum criteria for a 'Very High' consequence dam (MCE) should result in an annual probability of failure less than 1/100,000.

control, both of which form the basis for decisions on risk management.

8.2. Approaches to risk assessment

The simplest approach to introducing probabilistic methods into the evaluation of dam safety is to formulate safety guidelines in which the hazard to the dam is defined probabilistically as a function of the potential consequences of failure expressed in general terms. The probability of the failure is not evaluated. The dam safety guidelines formulated by the Canadian Dam Safety Association (CDSA) [53], are a good example of this approach. These guidelines have been adopted nationally. The CDSA recommendations on hazards specifications are outlined in Table 2 as a function of three categories of consequences of failure. The categories are defined in Table 3. The procedure for safety analysis of dams, once the seismic hazard is selected, follow conventional deterministic procedures such as stability calculations based on limit equilibrium and finite element methods. However, for High Consequence Dams in moderate to high seismic zones, seismic response and displacement analyses should be considered.

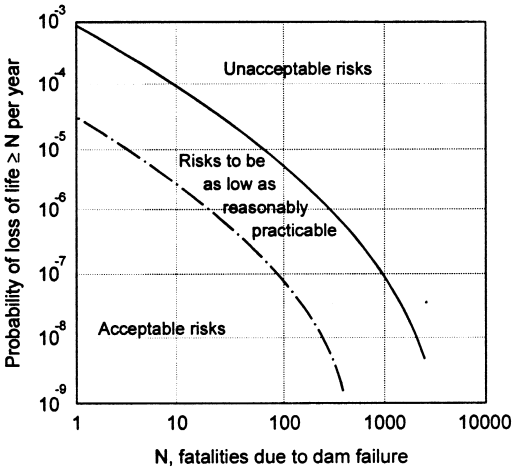

Fig. 19. ANCOLD societal risk criteria (from International Journal on Hydropower and Dams [60] with permission).

The Australian National Committee on Large Dams (ANCOLD) has been in the forefront in promoting formal risk assessment. In 1994, ANCOLD released its guidelines on risk assessment [54]. Some key elements of their guidelines as follows:

- Ensure that new dams, and dams being upgraded, satisfy the societal risk criterion given by the lower curve in Fig. 19.
- Ensure that existing dams satisfy the societal risk criterion given by the upper curve of Fig. 19, but carefully consider the principle that the risk be as low as reasonably possible.
- Ensure that a dam complies with both individual risk and societal risk criteria. In assessing compliance with individual and societal risk criteria, use a recognized methodology, such as the procedures set out by the US Bureau of Reclamation to estimate expected loss of life.

Note the crucial difference between formal risk assessment and the standards approach. The probabilities are now specified for the consequences, whereas in the standard approach, the emphasis is on the probability of the hazard.

8.3. Framework for risk assessment

The framework for formal risk assessment defines how to go from probabilistic specification of seismic hazard to the determination of the probabilities associated with different levels of consequences. The form of the framework depends on the potential failure modes of the dam. An example is presented in Fig. 20 from a paper by Lee et al. [55], which describes how the probability of different levels of post-liquefaction damage and consequences were assessed for Keenleyside Dam in British Columbia.

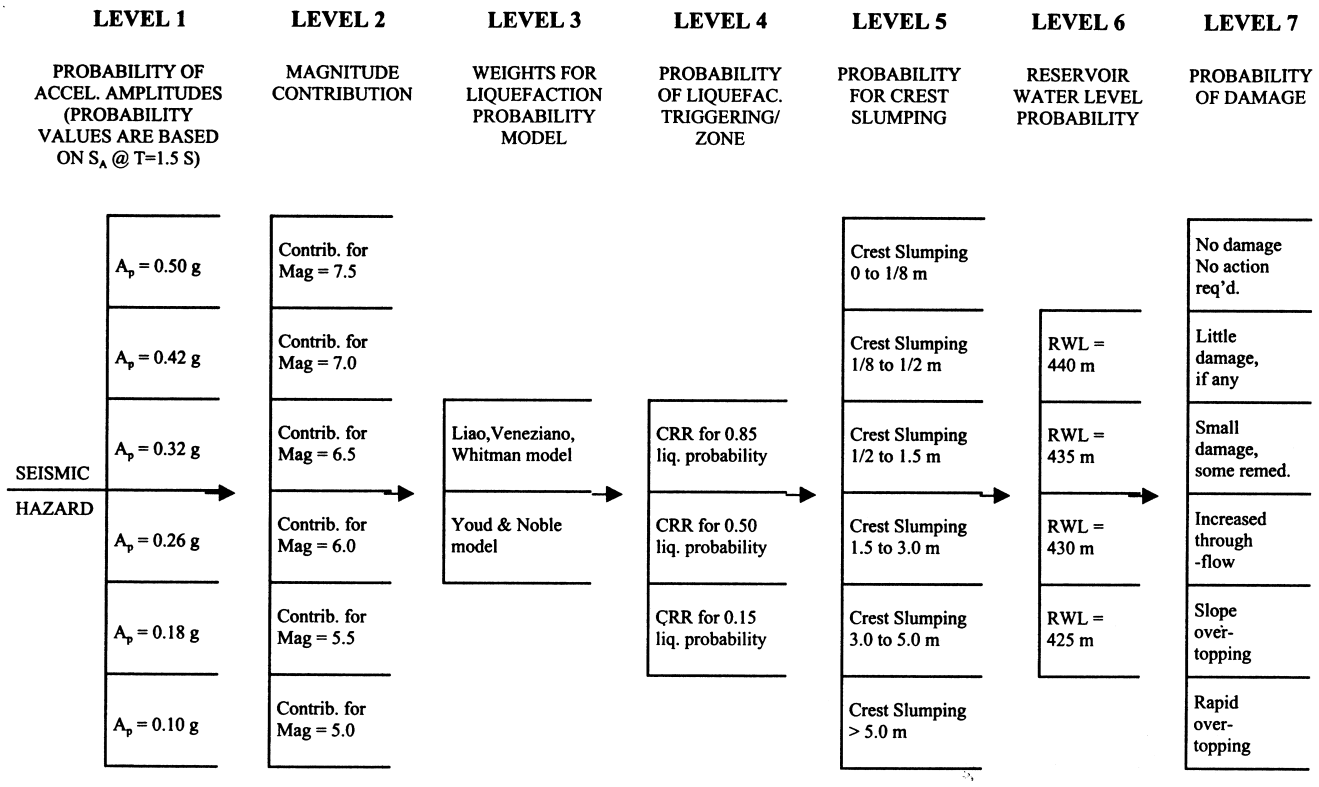

Fig. 20. Event tree used for the probability of liquefaction-failure (after Lee et al. [55]).

The first step is to specify the seismic hazard in Level 1 (Fig. 20). A range of shaking intensities is specified by peak ground accelerations. Each level of acceleration has its probability of exceedence. The potential for liquefaction, all other things being equal, depends on the duration of strong shaking. Duration is represented by the earthquake magnitude in the techniques used in engineering practice for assessing liquefaction potential [31,36]. Therefore, the magnitudes contributing most to the specified levels of shaking are obtained from a conventional seismic hazard assessment using a program such as EZ-FRISK 4.0 [56], which allows de-aggregation of the magnitudes contributing most to each level of seismic risk. On this basis, the magnitudes in Level 2 can be obtained. Level 3 in the event tree is the designation of the liquefaction model to be used in the analysis. Liao et al. [57] and Youd and Noble [58], using the database for the deterministic models, have developed charts that allow the estimation of the probability of liquefaction for a given level of shaking and a given level of liquefaction resistance to cyclic loading (CRR) specified by data from Standard Penetration Tests (SPT) or Cone Penetration Test (CPT). In the Keenleyside study, only the Liao et al. [57] probability model was actually used. If both models had been used, then weighting factors should be assigned to each. Cyclic resistance ratios, CRR, with probabilities of liquefaction of 0.85, 0.50 and 0.15 are used to assess the potential damage to the dam in terms of displacements such as loss of freeboard (crest slumping). These analyses are carried out by finite element analyses using post-liquefaction stress–strain-strength properties in the liquefied soils.

Six different levels of crest slumping are used to characterize the potential performance of the dam. At this stage, the conditional probabilities of these different levels may be introduced, based on computed response data and taking into account potential variations in properties of the materials, uncertainties in the analysis procedure itself, and the exercise of judgement. The definition of performance is a very critical part of the entire process. A simple criterion based on safety of factor against slope failure has been found to be unsatisfactory [55,59]. The probabilities based on such a narrow criterion appear to be overly sensitive to some details of the analyses.

The next step is evaluating the consequences. The consequences of the loss of freeboard associated with crest slumping obviously depends on the level of the reservoir. The probability of the reservoir being at specific levels can be calculated from the long-term records of reservoir operation, and consequently, probabilities can be assigned to the reservoir level being at a number of representative stages, as shown in Fig. 20. Judgements must now be made of the damage potential for the different combinations of crest settlement and reservoir level. This is the difficult part and requires expert judgement to assign subjective probabilities.

Whatever reservations one may have about the

probability of the various consequences derived from a risk assessment analysis, it is clear that constructing the event tree forces one to think in a very detailed way about the process by which failure develops in the dam, and therefore, it contributes to a deep understanding of how the dam is likely to behave. This is a very positive benefit of any well-conducted risk assessment study.

Acknowledgements

The Kushiro study was conducted in collaboration with Prof. Y. Sasaki of Hiroshima University.

References

[1] Somerville PG. Emerging art: earthquake ground motion. In: Dakoulas P, Yegian M, Holtz RD, editors. Proc Geotechnical Earthquake Engineering in Soil Dynamics III, Geotechnical Special Publication No. 75, vol. 1. ASCE, 1998. p. 1–38.

[2] SSA. Seismol Res Lett [special issue]. Seismol Soc Am 1997;68(1).

[3] Eurocode 8. Earthquake resistant design of structures. Commission of European Communities Tech. Committee CEN/TC250. 1993.

[4] ICBO. Uniform building code, vol. 2. Structural engineering design provisions. International Conference of Building Officials, Whittier, CA. 1997.

[5] Abrahamson NA, R R, Youngs A. stable algorithm for regression analysis using the random effects model. Bull Seismol Soc Am 1992;82:505–10.

[6] Youngs RR, Abrahamson NN, Makdisi FI, Sadigh K. Magnitude-dependent variance of peak ground acceleration. Bull Seismol Soc Am 1995;85:1161–76.

[7] Somerville PG, Sato T. Correlation of rise time with the style-of-faulting factor in strong ground motions. Seismol Res Lett 1998:153pp (abstract).

[8] Somerville PG, Greaves RL. Strong ground motions of the Kobe, Japan earthquake of January 17, 1995, and development of a model of forward rupture directivity applicable in California. Proc. Western Regional Tech. Seminar on Earthquake Eng. for Dams. Assoc. of State Dam Safety Officials, Sacramento, CA, April 11–12, 1996.

[9] Abrahamson NA, Silva WJ. Empirical duration relations for shallow crustal earthquakes. Written communication, 1997.

[10] Graves RW, Pitarka A, Somerville PG. Ground motion amplification in the Santa Monica area: effects of shallow basin edge structure. Submitted for publication.

[11] Abrahamson NA. Spatial variation of multiple support inputs. Proc. First US Symp. Seism. Eval. Retrofit Steel Bridges, UC, Berkeley, October 18, 1993.

[12] Naeim F, Lew M. On the use of design spectrum compatible motions. Earthquake Spec 1995;II(1):111–28.

[13] McGuire RK. Probabilistic seismic hazard analysis and design earthquakes: closing the loop. Bull Seismol Soc Am 1995;86:1275–84.

[14] Abrahamson NA, Schneider JF, Stepp JC. Empirical spatial coherency functions for applications to soil–structure interaction analyses. Earthquake Spec 1992;7:1–27.

[15] Seed HB, Lee KL, Idriss IM, Makdisi FF. The slides in the San Fernando Dams during the earthquake of February 9, 1971. J Earthquake Engng Division, ASCE 1975;101(GT77):651–68.

[16] Finn WD. Liam. Seismic safety evaluation of embankment dams. Proc., Int. Workshop on Dam Safety Evaluation, vol. 4, Grindewald, Switzerland, 26–28 April, 1993. p. 91–135.

[17] Seed HB, Seed RB, Harder Jr, LF, Jong H-L. 1989. Re-evaluation of the Lower San Fernando Dam, Report No. 2. Examination of the post-earthquake slide of February 9, 1971. Dept. of the Army, US Army Corps of Engineers, Washington, DC 20314-1000, 1989.

[18] Newmark N. Effects of earthquakes on dams and embankments. Geotechnique 1965;15(2):139–60.

[19] Finn WD, Liam. Dynamic analysis in geotechnical engineering. Proc., Earthquake Engineering and Soil Dynamics II — Recent Advances in Ground Motion Evaluation, ASCE Geotechnical Engineering Division, Park City, Utah, 1988. p. 523–91.

[20] Marcuson WF, Hynes ME, Franklin AG. Seismic stability and permanent deformation analyses: the last twenty five years. In: Seed RB, Boulanger RW, editors. ASCE Specialty Conference on Stability and Performance of Slopes and Embankments — II, Geotechnical Special Publication No. 31, vol. I. New York, NY: ASCE, 1992. p. 552–92.

[21] Finn WD, Liam, Yogendrakumar M, Yoshida N, Yoshida H. TARA-3: a program for nonlinear static and dynamic effective stress analysis. Soil Dynamics Group, University of British Columbia, Vancouver, BC, Canada, 1986.

[22] Martin GR, Finn WD, Liam, Seed HB. Fundamentals of liquefaction under cyclic loading. J Geotech Engng Div, ASCE 1975;101(GT5):423–38.

[23] Saada A, Bianchini GS, editors. Proceedings, International Workshop on Constitutive Equations for Granular Non-Cohesive Soils, Case Western Reserve University, Cleveland, Ohio July 22–24 Rotterdam: A.A. Balkema, 1987.

[24] Prevost JH. DYNAFLOW: a nonlinear transient finite element analysis program, Princeton University, Department of Civil Engineering, Princeton, NJ, 1981.

[25] Kawai T. Summary report on the development of the computer program DIANA — dynamic interaction approach and non-linear analysis. Science University of Tokyo, 1985.

[26] Roth WH. Evaluation of earthquake induced deformations of Pleasant Valley Dam. Report for the City of Los Angeles, Dames and Moore, LA, 1985.

[27] Moriwaki Y, Beikae M, Idriss IM. Nonlinear seismic analysis of the upper San Fernando Dam under the 1971 San Fernando Earthquake. Proc. 9th World Conf. on Earthquake Engineering, Tokyo and Kyoto, Japan, vol. III, 1988. p. 237–41.

[28] Itasca. FLAC (version 3.3) Itasca Consulting Group Inc, 708 South 3rd Street, Suite 310, Minneapolis, MN 55415, 1996.

[29] National Research Council. Liquefaction of soils during earthquakes. Report of Committee on Earthquake Engineering, Washington, DC, 1985.

[30] NCEER. Proceedings, Workshop on Evaluation of Liquefaction Resistance of Soils. Technical Report No. NCCER-97-0022. National Center for Earthquake Engineering Research, University of Buffalo, Buffalo, New York, 1997.

[31] Seed HB, Tokimatsu K, Harder LF, Chung RM. Influence of SPT procedures in soil liquefaction resistance evaluations. J Geotech Engng 1985;111(12):1425–45.

[32] Robertson PK, Fear CE. Liquefaction of sands and its evaluation. Proceedings, 1st Int. Conf. on Earthquake Geotechnical Engineering, Tokyo, Japan, 1995.

[33] Robertson PK, Woeller DJ, Finn WD, Liam. Seismic cone penetration test for evaluating liquefaction potential under cyclic loading. Can Geotech J 1992;29(4):686–95.

[34] Idriss IM. Submission to NCEER 1997 Report. In: Youd TL, Idriss IM, editors. NCEER. Proceedings, Workshop on Evaluation of Liquefaction Resistance of Soils. Technical Report No. NCCER-97-0022. National Center for Earthquake Engineering Research, University of Buffalo, Buffalo, NY, 1997.

[35] Ambraseys NN. Engineering seismology. Earthquake Engng Struct Dynam 1988;17:1–105.

[36] Seed HB, Idriss IM. Ground motions and soil liquefaction during earthquakes. Earthquake Engineering Research Institute, Oakland, CA, 1982.

[37] Seed HB. Design problems in soil liquefaction. J Geotech Engng, ASCE 1987;113(7):827–45.

[38] Seed RB, Harder Jr LF. SPT-based analysis of cyclic pore pressure generation and undrained residual strength. In: Duncan JM, editor. Proceedings, H. Bolton Seed Memorial Symposium, University of California, Berkeley, May 9–11, vol. 2. 1990. p. 351–76.
[39] National Science Foundation (NSF). Post-liquefaction shear strength of granular soils. In: Stark TD, Kramer SL, Youd TL, editors. Proceedings of Workshop on Post-Liquefaction Shear Strength of Granular Soils, April 18–19, 1997.
[40] Castro G. Liquefaction of Sands, Harvard Soil Mechanics Series No. 81. Cambridge, MA: Pierce Hall, 1969.
[41] Poulos SJ, Castro G, France W. Liquefaction evaluation procedure. J Geotech Engng Div, ASCE 1985;111(6):772–92.
[42] Vaid YP, Sivathayalan S, Stedman D. Influence of specimen reconstituting method on the undrained response of sand. Submitted for publication.
[43] Vaid YP, Stedman D, Sivathayalan S. Static shear, confining pressure coupling effects on liquefaction of sand. To be submitted for publication.
[44] Uthayakumar M, Vaid YP. Static liquefaction of sand under multiaxial loading. Can Geotech J 1998;35(2):273–83.
[45] Yoshimine M, Ishihara K, Vargas W. Effect of principal stress direction and intermediate principal stress on undrained shear behaviour of sand. Soils and Foundations, Japan Soc Soil Mechanics Foundation Engng 1998;38(3):179–88.
[46] Finn WD, Liam. Analysis of post-liquefaction deformations in soil structures (Invited Paper). In: Duncan JM, editor. Proc H. Bolton Seed Memorial Symposium, University of California, Berkeley, May 9–11, vol. 2. Vancouver: Bi-Tech Publishers, 1990. p. 291–311.
[47] Finn WDL, Ledbetter RH, Fleming Jr RL, Forrest TW, Stacy ST. Stabilization of an earth dam using driven prestressed concrete piles. Int J Earthquake Engng, London 1998;2(2):173–95.
[48] Byrne PM, Imrie AS, Morgenstern NR. Results and implications of seismic performance studies for Duncan Dam. Can Geotech J 1994;31(6):979–88.
[49] Vaid YP, Thomas J. Post-liquefaction behaviour of sand. Proc. 13th International Conference on Soil Mechanics and Foundation Engineering, New Delhi, vol. 3, 1994. p. 1305–10.
[50] Vaid YP, Sivathayalan S. Static and cyclic liquefaction potential of fraser delta sand in simple shear and triaxial tests. Can Geotech J 1996;33(2):281–9.
[51] Ledbetter RH, Finn WD, Liam. Development and evaluation of remediation strategies by deformation analyses. Proceedings, Special Technical Publication, Geotechnical Practice in Dam Rehabilitation, ASCE, April 15–28, 1993.
[52] Finn WD, Liam, Yogendrakumar M. TARA-3FL: a program for analysis of flow deformations in soil structures with liquefied zones. Soil Dynamics Group. Department of Civil Engineering, University of British Columbia, Vancouver, BC, 1989.
[53] CDSA. Dam safety guidelines. Canadian Dam Safety Association, P.O. Box 4490, South Edmonton Postal Station, Edmonton, Alberta, Canada T6E 4X7.
[54] McDonald LA. Status of risk assessment of dams in Australia. Proc., International Workshop on Risk Based Dam Safety Evaluations, Trondheim, Norway. Norwegian National Committee of the International Committee on Large Dams, 1997.
[55] Lee MK, Lum KY, Hartford DND. Calculation of the seismic risk of an earth dam susceptible to liquefaction. Submitted for publication.
[56] Risk Engineering Inc. EZ-FRISK computer program 4.0. 4155, Dowley Avenue, Suite A, Boulder, CO 80303, 1997.
[57] Liao SSC, Veneziano D, Whitman RV. Regression models for evaluating liquefaction probability. J Geotech Engng, ASCE 1988;114(4):389–411.
[58] Youd TL, Noble SK. Magnitude scaling factors. In: Leslie Youd T, editor. Draft Report, NCEER Workshop on Evaluation of Liquefaction Resistance, Brigham Young University, Provo, Utah.
[59] Whitman RV. Evaluating calculated risk in geotechnical engineering (17th Terzaghi Lecture). J Geotech Engng ASCE 1984;110(2):145–88.
[60] International Journal on Hydropower and Dams. Editorial Reports on Seismic Risk. 51(1 and 2). Aqua-Media, Sutton, Surrey, UK, 1999.